Available online at www.sciencedirect.com

ScienceDirect

Procedia Structural Integrity 2 (2016) 3018–3025

Structural Integrity Procedia

www.elsevier.com/locate/procedia

21st European Conference on Fracture, ECF21, 20-24 June 2016, Catania, Italy

Stage I fatigue cracking in MAR-M 247 superalloy at elevated temperatures

Miroslav Šmíd[a]*, Pavel Hutař[a,b], Vít Horník[c], Karel Hrbáček[d], Ludvík Kunz[b]

[a]*CEITEC IPM, Žižkova 22, Brno, 616 62, Czech Republic*
[b]*Institute of Physics of Materials, AS CR, Žižkova 22, Brno, 616 62, Czech Republic*
[c]*Brno University of Technology, Technická 2896/2, Brno 616 69, Czech Republic*
[d]*PBS Velká Bíteš, a.s., Vlkovská 279, Velká Bíteš, 595 12, Czech Republic*

Abstract

Nickel base superalloys exhibit fatigue fracture behavior with features of brittle-like cleavage cracking under high cycle fatigue loading at temperatures up to approximately 800 °C. This specific fracture behavior was already documented in several studies, but a possible mechanism of fatigue crack propagation under this mode has not been made completely clear yet. The aim of this paper is to put more light on the phenomenon by using advanced electron microscopy techniques like electron back-scattered diffraction (EBSD) and focused ion beam (FIB) sectioning. Fractured specimens after high cycle fatigue tests were thoroughly examined with the aim to localize the fatigue crack initiation sites and accompanying features of the fatigue crack propagation. Several specimens were cross-sectioned in order to characterize active slip systems, cyclic plastic deformation localization and fatigue crack propagation. Dislocation structures were studied by transmission electron microscopy (TEM).

Peer-review under responsibility of the Scientific Committee of ECF21.

Keywords: Superalloy; High cycle fatigue; Elevated temperature; MAR-M 247; Fatigue crack initiation

1. Introduction

Nickel base superalloys are materials which possess excellent high temperature strength, resistance to oxidation and good creep resistance. They are widely used in electric power generation, aerospace and automotive industry for design and production of various components which are subjected to a combination of high temperature exposure

* Corresponding author. Tel.: +420 532 290 362.
E-mail address: smid@ipm.cz

Peer review under responsibility of the Scientific Committee of ECF21.
10.1016/j.prostr.2016.06.378

and mechanical loading. Majority of mechanical loading has a cyclic character and therefore fatigue endurance of the superalloys is one of the key material properties. Despite the superalloys have been a subject of interest of material science society for decades there are still unanswered questions regarding some aspects of fatigue.

The stage I cracking is one of these not fully explored areas. Despite this failure mode has been known and studied for decades it is still not completely understood how fatigue crack initiates and propagates. The occurrence of the stage I crack initiation and propagation depends on several conditions like temperature, frequency or strain rate of the loading. These conditions were broadly described by Leverant and Gell (1975). Generally, increasing frequency of fatigue loading promotes stage I cracking while increasing temperature promotes stage II cracking, typical for fatigue loading. As an example of this variability, work of Yi et al. (2007) proved that this mode of cracking occurs even at high temperature under ultrasonic loading but other study of MacLachlan and Knowles (2001) has shown that at roughly the same temperature under low frequency testing results in a typical stage II cracking. Fatigue fracture surface after this mode of crack propagation is rugged with numerous facets. Fracture surface with such features has almost brittle-like character without any noticeable signs of fatigue crack propagation like beach marks and striations. From character of fracture surface and closer observations of facets it is obvious that the stage I cracking is significantly crystallographically dependent and the crack propagation is along {111} type slip planes according to numerous studies (Liu et al. (2011), Gell and Leverant (1968), Miao et al. (2012)).

In our previous studies, Šmíd et al. (2014 and 2016), high cycle fatigue (HCF) performance of the MAR-M 247 superalloy was studied extensively in temperature range from 650 to 950 °C. Special emphasis was put on fractography analysis and the change of appearance of the fracture surface with increasing temperature. The present study focuses on investigation of failed specimens after fatigue tests just at 650 and 800 °C, that means in the temperature range where the stage I cracking mode is employed in significant extent. The aim is to elucidate some aspects of this stage I crack initiation and propagation. It is well known that distribution of cyclic plastic deformation during HCF loading is localized into narrow slip bands. In order to study and observe such fine structural features advanced electron microscopy techniques like electron channeling contrast imaging (ECCI) or TEM lamella preparation by FIB were employed. Therefore, complex characterization of the particular grain was possible to carry out along with TEM observation from an area of interest. The results are discussed taking previous studies into account.

2. Experimental

Experimental material, the MAR-M 247 superalloy, was provided by the company PBS Velká Bíteš, a.s. in the form of pre-cast rods which were used for fabrication of cylindrical specimens. The chemical composition of the alloy is shown in Table 1. The pouring temperature of the melt into the mold was 1400 ± 15 °C. The alloy was processed by hot isostatic pressing (HIP) procedure (1200 °C / 4 h, 100 MPa). Subsequently, two-step heat treatment followed consisting of solution annealing at 1200 °C for 2 hours and precipitation annealing at 870 °C for 24 hours. Resultant structure of the alloy (see Fig. 1) is coarse dendritic with average grain size of 0.8 mm (determined by linear intercept method), although large grains over 3 mm occur frequently. Numerous casting defects were detected predominantly in interdendritic areas. Their typical size was around 400 μm. The strengthening phase γ′ with the volume fraction around 60 % is homogeneously distributed in the γ matrix. Areas of fine γ′ precipitates with mostly cuboidal shape (edge size 0.4 μm) are often surrounded by areas of coarse γ′ precipitates (1.6 μm in diameter) of more complicated morphology. Numerous carbides and eutectics γ / γ′ were found in the interdendritic and grain boundary areas. These particles accommodate a part of alloying elements like Ti, Ta, Hf and W.

Table 1. Chemical composition of the MAR-M 247 superalloy in wt. %.

C	Cr	Mo	Al	Ti	Ta	W	Co	Nb	Br	Hf	Ni
0.15	8.37	0.67	5.42	1.01	3.05	9.92	9.91	0.04	0.015	1.37	bal.

A resonant testing machine with 100 kN force range was used for fatigue tests under load control in fully reversed loading (stress ratio R = -1). The frequency of cyclic loading was around 120 Hz. Cylindrical specimens with a gauge length of 8 mm in diameter and 23 mm in length were used for experimental determination of the fatigue life. The temperature of testing was provided by a furnace with resistance heating. Test temperatures 650 and 800 °C were chosen for this study. All tests were done in laboratory air. A drop of test frequency by 5 Hz or specimen rupture were adopted as conditions for test termination. The fatigue limit, σ_f , was defined as the stress amplitude at which a minimum of three specimens reached $2x10^7$ cycles without failure. The fracture surfaces and specimen cross-sections were investigated by scanning electron microscope (SEM) Tescan Lyra 3XMU equipped with focused ion beam (FIB) column.

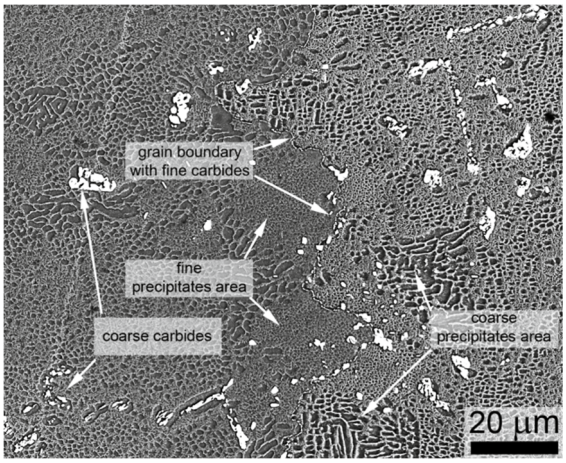

Fig. 1. Microstructure of MAR-M 247 superalloy.

Selected fractured specimens were sectioned in longitudinal direction to the loading axis by electro erosion cutting and carefully polished for further analysis of grains nearby the fracture surface. Several steps were done in order to acquire a complete characterization of material in an area of interest. Firstly, extensive EBSD analysis of grains nearby fracture surface was conducted. Recorded data were processed and slip systems of particular grain were identified and their Schmid factor (SF) calculated. Afterwards, fine observation of evidence of cyclic plastic deformation localization was done. There are two possible ways: (i) by electron channeling contrast imaging (ECCI) on polished samples or (ii) by backscattered electron imaging (BSE) on etched samples. In this study, first option was used predominantly. In rare cases, an etchant with solution of 40 ml HNO_3 and 30 ml HF was utilized. A sample prepared with preferentially etched precipitates provides higher contrast of structural features and the evidence of localization of plastic deformation into slip bands and shearing of precipitates is distinguishable. After an area of interest of further research was selected, a fabrication of TEM lamella was conducted in order to analyze dislocation structure from particular area. The only possible way to fulfil this task is the FIB milling technique. The procedure itself consists of several processes where the most essential is the ion milling of lamella to required thickness, that is transparent for electrons. Lastly, final fine polishing with low energy ions (2-5 keV) is desirable to conduct in order to get best quality lamella with visible dislocation structure. This sequence of analysis and observations enabled complex characterization of the desired grain.

3. Results

Figure 2 shows S-N curves determined from HCF tests at 650 and 800 °C. Data points with arrows denote run-out specimens which reached at least $2x10^7$ cycles. Experimental data are burdened by significant scatter due to cast nature of the alloy. Despite the scatter and limited number of tests, distinct change in HCF performance can be seen between both temperatures. Lower fatigue limit, 190 MPa, was determined at 650 °C and also fatigue tests from area of finite fatigue life yield noticeably lower number of cycles to failure than HCF tests performed at 800 °C.

The fatigue limit of 220 MPa was determined for this temperature. The diagram also shows distinctively different slopes of both S-N curves.

Selected specimens were cross-sectioned along the loading axis with intention to study fatigue crack propagation. It was found out that it is possible to observe evidence of slip activity along active slip systems and also sheared precipitates. Figure 3 shows example of high slip activity along numerous slip planes inside of one grain.

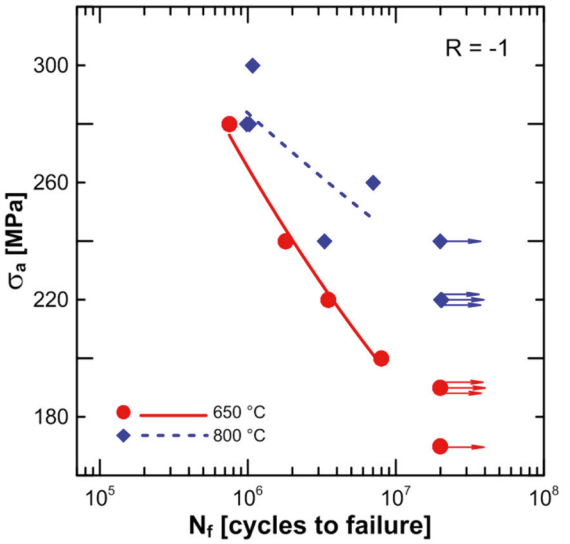

Fig. 2. Fatigue life curves at temperature 650 and 800 °C. Data points with arrow denote run-out specimens.

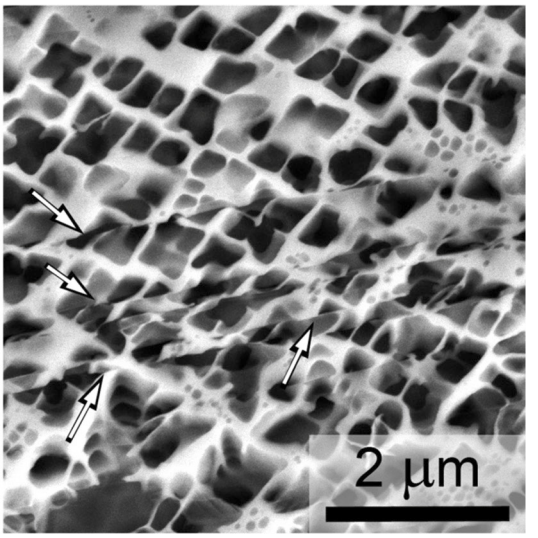

Fig. 3. Micrograph taken on axial section of specimen showing severe slip activity along slip plane with numerous sheared precipitates.

The above described characterization was employed on several cross sections. Figure 4 consists of four images illustrating particular stages of the investigation done on specimen after fatigue loading at 650 °C. Rugged fatigue fracture surface with large crystallographic facet and selected cross-section area is shown in Figure 4a. Fatigue crack initiation site was identified as a shrinkage pore which is highlighted by an arrow. The fatigue crack propagated into large neighboring grain with suitably oriented slip plane. Figure 4b presents the image of cross section sample with the EBSD analysis of grains in the vicinity of the crack in form of the inverse pole figure map. Analysis of recorded data enabled identification of slip planes. The stage I crack propagation across the grain no. 2 (featured with the facet) was along slip plane (111) with high Schmid factor. The crack propagated in the stage I mode across the whole grain. Evidence of localization of plastic deformation into slip band was found in the grain no. 3. From this area the TEM lamella was fabricated by FIB in perpendicular orientation to the slip band. Figure 4c was acquired during the milling process. The image showed that there is not only a slip plane with signs of significant slip activity but already a developed crack propagating in the stage I mode. STEM micrograph of the lamella is shown in Figure 4d. Observed dislocation structure has distinct planar alignment. Three slip systems were active in this particular grain while two of them had Schmid factor of similar value. Nevertheless, the crack propagated just along one of them, slip system $(\bar{1}11)$. Dislocation density outside of active slip planes was very low.

Figure 5 shows a set of images from similar characterization carried out on a specimen tested at 800 °C. Fatigue fracture surface is depicted in Figure 5a. Facet from the stage I crack propagation is in this case smaller due to smaller grain. Subsequent stage II crack propagation was more apparent and covered distinctively larger area of the fracture surface than after HCF tests at 650 °C. The fatigue crack initiated in area of a shrinkage pore nearby the grain no. 1 which is visible in inverse pole figure map of polished cross section sample (see Figure 5b). The crack propagated along suitably oriented slip plane (SF. = 0.492) in the stage I mode from the shrinkage pore across the grain no. 1 until it reached grain boundary. Fine observation revealed areas with evidence of high slip activity accompanied with sheared precipitates which are shown in Figure 5c. TEM lamella, depicted by arrows, was taken out from area perpendicular to the slip plane. TEM micrograph (see Figure 5d) shows well developed slip bands

along the slip system (111). In this particular case just one slip system was active probably due to its almost ideal orientation to the loading axis. Higher dislocation density was observed in channels of matrix and γ / γ′ interfaces. That was a distinct difference from the observed dislocation structure after HCF tests at 650 °C.

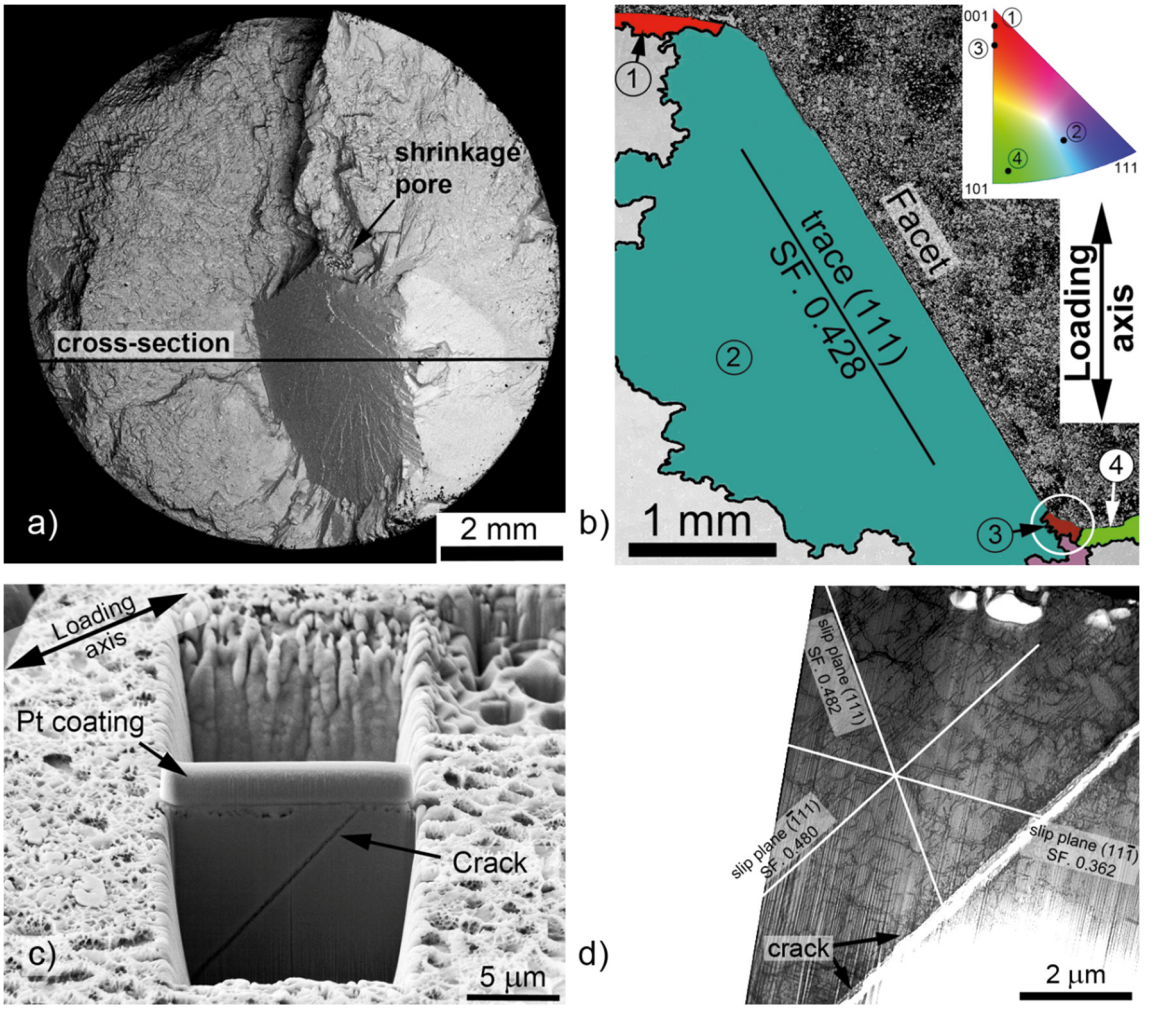

Fig. 4. Investigation of specimen cyclically loaded at 650 °C by σ_a = 240 MPa (N_f = 1.3x10^6 cycles): (a) fracture surface with shown area of section for further analysis; (b) inverse pole figure map showing some of grains in vicinity of fatigue crack. Crystallographic facet was identified as parallel to slip plane (111). The circle is showing an area of subsequent TEM lamella fabrication; (c) micrograph taken during TEM lamella fabrication with visible fatigue crack; (d) STEM image of lamella with the crack and multiple active slip planes.

ECCI image of the area in front of crack tip is shown in Figure 6. This imaging mode enabled to enhance the contrast of structural features and signs of slip activity in the slip plane of fatigue crack in front of the crack tip. The crack propagated strictly along slip plane (111) with Schmid factor of 0.487. Pronounced discontinuity of the crack tip was observed in the form of few elongated cavities which are isolated from well-developed and continuous crack. Furthermore, it was possible to observe that cyclic plastic deformation was accommodated in the slip plane already few micrometers in front of these vacancies.

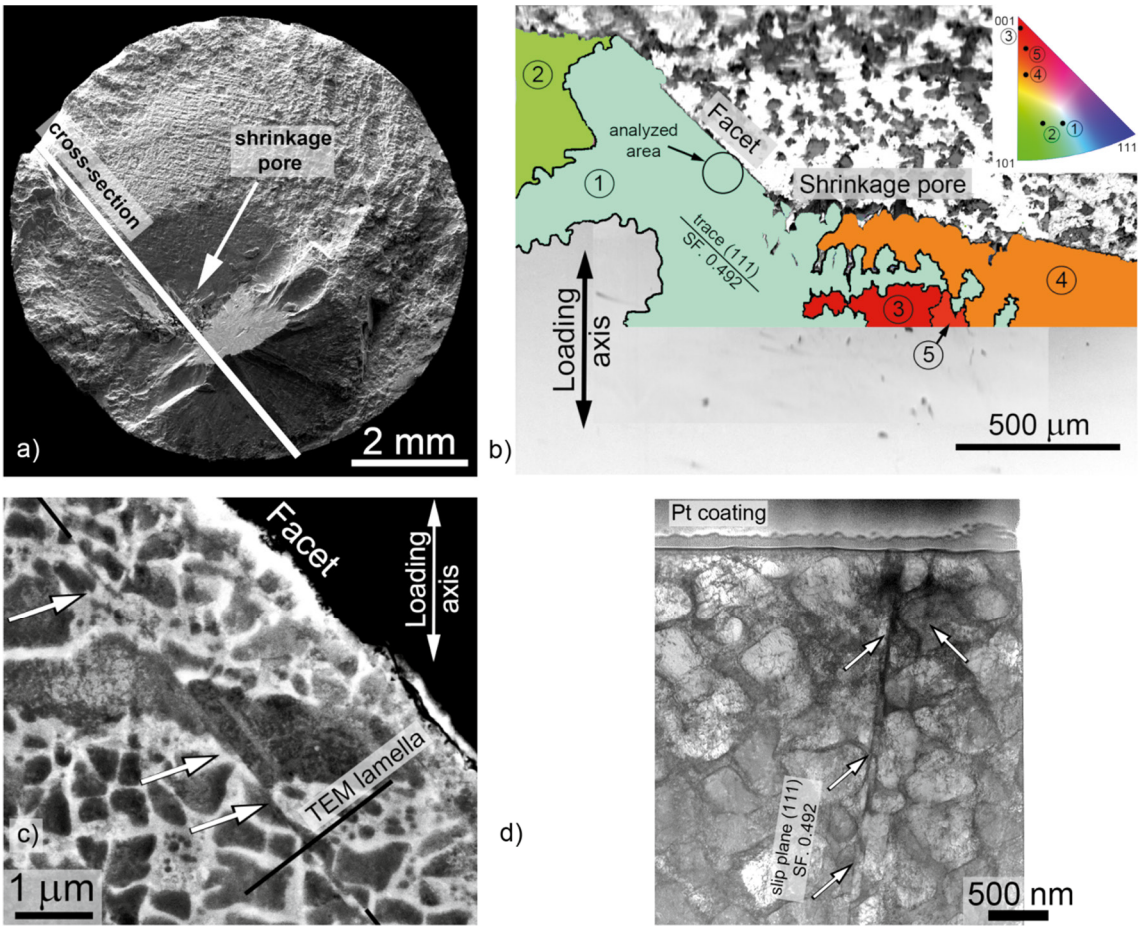

Fig. 5. Investigation of specimen cyclically loaded at 800 °C by σ_a = 280 MPa (N_f = 7.52x10^5 cycles): (a) fracture surface with shown area of section for further analysis; (b) inverse pole figure map showing some of grains in vicinity of fatigue crack. Crystallographic facet was identified as parallel to slip plane (111) with high Schmid factor. The circle indicates an area of further observations; (c) ECCI image of area chosen for TEM lamella fabrication. Arrows are showing slip band with visible shearing of precipitates along plane parallel with fracture facet; (d) TEM image of lamella with severe localization of plastic deformation into few slip planes.

4. Discussion

Presented S-N curves (Fig. 2) show noticeable difference in fatigue behavior of the MAR-M 247 alloy at 650 and 800 °C. Fatigue performance at 650 °C was worse and determined fatigue limit was lower than at 800 °C. The slopes of both curves indicate that different fatigue damage mechanism is dominant for each temperature. Fracture surfaces from tests at 650 °C suggest that strong crystallographic dependence and intense localization of cyclic plastic deformation results in dominant stage I fatigue crack initiation and propagation. Stress concentrators like shrinkage pores have a significantly higher influence on fatigue life under such conditions.

Despite the stage I facets occurred on fracture surfaces after tests at 800 °C their presence was reduced and the fatigue crack propagation was mostly in the stage II mode. According to these observations it can be deduced that thermally activated processes were more involved and therefore crystallographic dependency and strong localization of the plastic deformation become considerably weakened. This fact is in good agreement with our previous work Šmíd et al. (2014) and also other studies like Leverant and Gell (1975) or Crompton and Martin (1984). Consequently, the stress concentration on structural defects is less detrimental for fatigue life at 800 °C. Described difference in the fatigue life between both temperatures is diminishing with increasing stress amplitude. Therefore it can be supposed that the temperature dependence of the fatigue life would disappear in the region of

low cycle fatigue (i.e. less than 10^5 cycles), which is characterized by more homogeneous distribution of the cyclic plastic deformation in volume and less important role of structural defects.

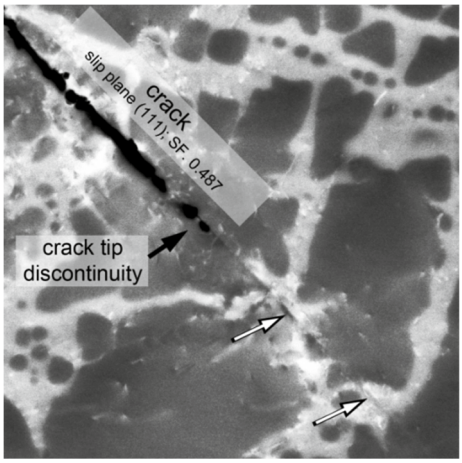

Fig. 6. ECCI image of crack tip. Evidence of pronounced slip activity along the slip plane is highlighted by arrows. Note that crack tip is discontinuous accompanied by some type of cavities.

The characterization of selected specimen cross-section after test at 650 °C (Fig. 4) confirmed that large stage I facet is parallel with one of the slip plane of type {111} with high Schmid factor. Shrinkage pore, which was found on fracture surface, acted like a stress concentrator which facilitated the localization of cyclic plastic deformation into the slip plane. This favorable combination of well oriented large grain and presence of significant shrinkage pore resulted in the stage I crack initiation. The detrimental effect of combined influence of structural features was already documented by Du et al. (2015) and also Miao et al. (2012). Moreover, favorably oriented large grain with several suitable slip planes can be considered even as a defect and critical place for HCF loading. The observed inhomogeneous dislocation structure is in good agreement with the character of the stage I cracking. Dislocation structure has significant planar alignment where most of dislocations are accommodated in several slip planes. This is characteristic for low stacking fault energy materials where cross slip of dislocations is difficult till the moment when thermally activated processes like diffusion and dislocation climb start to play more important role. The observation indicated that cyclic plastic deformation took place in a few slip systems simultaneously but one slip system finally prevails during cycling and the fatigue crack initiates just there. Similar characterization carried out on specimen after HCF test at 800 °C (Fig. 5) revealed the same mechanism of cyclic plastic deformation localization and fatigue crack propagation along slip plane (111) in the near vicinity of a shrinkage pore. TEM observation revealed well developed slip bands with signs of precipitate shearing along (111) plane and high dislocation density in matrix channels and along interfaces of matrix/precipitates. Thermally activated processes are more pronounced and cause higher dislocation mobility. Therefore they are not already restricted just into few preferred slip systems. That was a noticeable difference when compared to the dislocation structures after loading at 650 °C where majority of channels and interfaces were mostly without dislocations. Similar temperature dependent changes of dislocation structure were mentioned already by Gell and Leverant (1975) or Zhaokuang et al. (2008).

Fine SEM observation in ECCI mode carried out in areas of stage I crack tips (Fig. 6) revealed that plastic zone is predominantly confined just into the same slip system along which the crack propagated. This is in good agreement with our TEM observations. Vacancies similar to those observed in this alloy were already reported in the study of Weicheng et al. (1987) where it was proposed that they are the consequence of cyclic plastic deformation along slip band. Our observation leads to the same conclusion. Moreover, it can be supposed that vacancies are in some way promoting the stage I crack propagation. Further investigations has to be done to clarify this possible mechanism.

5. Conclusions

- Fatigue performance varies significantly between temperatures 650 and 800 °C. Different slope of S-N curves indicates different dominant damage mechanisms operating in the material during the cyclic loading.
- Fatigue crack propagation at 650 °C is predominantly in the stage I mode featured by crystallographic facets along the slip planes of type {111}. Planar alignment of dislocation structures illustrates restriction of cyclic plastic deformation into several {111} slip planes with high Schmid factor.
- Distinct planar alignment of dislocation structure was identified in reduced extend in specimens after cyclic loading at 800 °C. Apart from that, high dislocation density was found in the channels of matrix and interfaces γ / γ'. That is evidence of reduced crystallographic dependency of cyclic plastic deformation and higher dislocation mobility due to thermally activated processes. Therefore the stage I crack propagation was observed just in early stages of fatigue life followed by classic stage II mode.
- Contribution of secondary slip systems into fatigue crack propagation seems to be minimal even though TEM observation showing high activity on them. Fatigue crack propagation is promoted by high slip activity along single slip plane accompanied with fine cavities in front of the crack.

Acknowledgement

Authors of the article are grateful for financial support by the Project TA04011525 Technological Agency of the Czech Republic. The research was conducted in the frame of IPMinfra supported through project No. LM2015069 of MEYS. This work was also realized in CEITEC - Central European Institute of Technology - with research infrastructure supported by the project CZ.1.05/1.1.00/02.0068 financed from European Regional Development Fund.

References

Crompton, J.S., Martin, J.W., 1984. Crack Growth in a Single Crystal Superalloy at Elevated Temperature. Metallurgical Transactions A 15, 1711-1719.

Du, B., Yang, J., Cui, C., Sun, X., 2015. Effect of grain size on the high-cycle fatigue behavior of IN792 superalloy. Materials and Design 65, 57-64.

Gell, M., Leverant, G.R., 1968. The Fatigue of the Nickel-Base Superalloy, Mar-M200, in Single-Crystal and Columnar-Grained Forms at Room Temperature. Transactions of the metallurgical society of AIME 242, 1869-1879.

MacLachlan, D.W., Knowles, D.M., 2001. Fatigue behaviour and lifing of two single crystal superalloys. Fatigue & Fracture of Engineering Materials & Structures 24, 503-521.

Miao, J., Pollock, T.M., Jones, J.W., 2012. Microstructural extremes and the transition from fatigue crack initiation to small crack growth in a polycrystalline nickel-base superalloy. Acta Materialia 60, 2840-2854.

Leverant, G.R., Gell, M., 1975. The Influence of Temperature and Cyclic Frequency on the Fatigue Fracture of Cube Oriented Nickel-Base Superalloys Single Crystals. Metallurgical Transactions A 6, 367-371.

Liu, L., Husseini, N.S., Torbet, C.J., Lee, W.-K., Clarke, R., Jones, J.W., Pollock, T.M., 2011. In situ synchrotron X-ray imaging of high-cycle fatigue crack propagation in single-crystal nickel-base superalloy. Acta Materialia 59, 5103-5115.

Šmíd, M., Kunz, L., Hutař, P., Hrbáček, K., 2014. High cycle fatigue of nickel-based superalloy MAR-M 247 at high temperatures. Proceedia Engineering 74, 329-332.

Šmíd, M., Horník, V., Hutař, P., Hrbáček, K., Kunz, L., 2016. High Cycle Fatigue Damage Mechanisms of MAR-M 247 Superalloy at High Temperatures. Transactions of Indian Institute of Metals 69, 393-397.

Yi, J.Z., Torbet, C.J., Feng, Q., Pollock, T.M., Jones, J.W. 2007. Ultrasonic fatigue of a single crystal Ni-base superalloy at 1000 °C. Material Science and Engineering A 443, 142-149.

Zhaokuang, C., Jinjiang, Y., Xiaofeng, S., Hengrong, G., Zhuangqi, H., 2008. High cycle fatigue behavior of a directionally solidified Ni-base superalloy DZ951. Material Science and Engineering A 496, 355-361.